Numerical Modelling of Heat Generated by Electroosmotic Flows in Micro-Channels

P. NITHIARASU* and P.F. ENG

* Corresponding author: Tel.: ++44 (0)1792 513267; Fax: ++44 (0)1792 295676; Email: P.Nithiarasu@swansea.ac.uk
School of Engineering, Swansea University, UK

Abstract In this paper, numerical modeling of Joule heating in electroosmotic flows is described in some detail. The finite element method is used for the spatial discretization along with the characteristic based split (CBS) time discretization. A new non-dimensional scaling is also introduced. In addition to standard problems of micro channel flows, flow and heat generation in a T-mixer are also discussed in this paper.

Keywords: Micro channel flows, electroosmosis, heat generation, biomedical applications, numerical modeling.

1. Introduction

Electro-osmotic flow (EOF) has been a basis for designing certain types of biomedical and micro-cooling devices for several years. EOF is used as pumping, valving, mixing, splitting and delivering mechanisms in "lab-on-chip" devices for biological and chemical analyses and medical diagnoses (Bianchi et al., 2000; Dutta et al. 2001). It is also used in cooling of electronic equipment (Jiang et al. 2002; Zeng et al. 2001). In both these applications, Joule heating can be a factor in the design. In biological applications, increased use of low cost, but poor heat conducting materials (Erickson 2003), poses the problem of heat dissipation. In electronic cooling applications, Joule heating increases the temperature of the coolant and imposes an extra burden on the cooling system. Thus, Joule heating and it's the dissipation are of one of the major challenges currently faced by heat transfer engineers. Numerical modelling of Joule heating helps to estimate the approximate increase in the electrolyte temperature and thus leads to a better device design to dispose the heat generated.

In biological (Erickson 2003) and other applications (Arnold, 2007), the presence of conjugate heat transfer is apparent. Thus, a numerical model should include strategies for dealing with the heat conduction in the surrounding solid.

A small number of modelling studies have been reported on Joule heating in EOF and different non-dimensional scalings have been adopted in these studies (Zhao et al. 2002; Erickson, 2003; Tang et al. 03a; Tang et al. 2004a, Tang et al. 2004b; Xuan et al. 2004; Huang et al. 2006; Tang et al. 2006a; Chein et al. 2006; Tang et al. 2007). Though the scalings used in these works are correct, some of them may not always be convenient and they are not sufficiently general to use. Thus, we use a non-dimensional scaling scheme that is often adopted in the natural convection and conjugate heat transfer studies (Nithiarasu et al. 1998; Nithiarasu, 2008; Nithiarasu and Lewis, 2008). This scaling is general and it does not change with the boundary conditions or other variable parameters.

The objective of the present work is thus to introduce the new non-dimensional scales and also to solve the heat generation problem using the implicit-explicit approach (Singh et al., 2008). Section 2 introduces the governing equations and the non-dimensional scales. The numerical algorithm is briefly presented in Section 3. Sections 3, 4 and 5 provide some examples to demonstrate the non-dimensional scales and the numerical algorithm proposed.

2. Governing Equations and Numerical Algorithm

An electric field is defined as electric force per unit charge. The strength of such a field is determined from the divergence of the electric field as,

$$\nabla.\lambda\mathbf{E} = 0 \tag{1}$$

where λ is the electrical conductivity and the electric field, E is defined as,

$$\mathbf{E} = -\nabla\phi \tag{2}$$

where ϕ is the electric potential. Thus, the equation governing the external electric potential may be written as,

$$\nabla.(\lambda\nabla\phi) = 0 \tag{3}$$

The electric field generated by uneven distribution of ions near a solid wall may be expressed using a Poisson equation. Since this process is of a generation type, the equation involves a source term that is a function of the charge density, i.e.,

$$\nabla.(\varepsilon\nabla\psi) = -\frac{\rho_E}{\varepsilon_0} \tag{4}$$

The charge density, ρ_E is related to the ion concentration. Often, a Boltzmann type distribution is assumed for the ion concentration. Assuming a symmetric electrolyte, the charge density may be written as

$$\rho_E = -2n_0 ze\sinh\left(\frac{ze\psi}{k_b T}\right) \tag{5}$$

Thus, the Poisson-Boltzmann equation governing the electric potential may be written as

$$\nabla.(\varepsilon\nabla\psi) = \frac{2n_0 ze}{\varepsilon_0}\sinh\left(\frac{ze\psi}{k_b T}\right) \tag{6}$$

The artificial compressibility form of the modified Navier-Stokes equations written in a non-conservation form may be written as follows:

Continuity equation:

$$\frac{1}{\beta^2}\frac{\partial P}{\partial t} + \rho\nabla.\mathbf{u} = 0 \tag{7}$$

Momentum equation:

$$\rho\left(\frac{\partial u}{\partial t} + \mathbf{u}.\nabla\mathbf{u}\right) = -\nabla P + \nabla.\tau - \rho_E\mathbf{E} \tag{8}$$

where

$$\tau = \mu\left(\nabla\mathbf{u} + \nabla\mathbf{u}^T\right) \tag{9}$$

and the energy equation is

$$\rho c_p\left(\frac{\partial T}{\partial t} + \mathbf{u}.\nabla T\right) = \nabla.\left(k\nabla T\right) + \lambda\left|\mathbf{E}\right|^2 \tag{10}$$

where the last term in the above equation represents Joule heating. Equations (1), (6), (7), (8) and (10) along with appropriate boundary and initial conditions, govern EOF through micro-channels. It is also important to note that the electrolyte properties, such as electrical conductivity (λ), dielectric constant (ε), viscosity (μ) and thermal conductivity (k) can also be a function of temperature.

2.1 Governing Equations

Unlike the previously used scales, the following non-dimensional scales are consistent and general. Since actual flow velocities are not known *a priori*, calculating a Reynolds number *a priori* is therefore not possible. Thus, the scales should be selected in such a way as to avoid introducing a Reynolds number into the non-dimensional form. It is also important to have a consistent scale for both the external potential and the potential generated by the clustering of ions close to the walls. Bearing in mind the above points, the following scales are selected to non-dimensionalise the governing equations.

$$\phi^* = \frac{\phi}{\phi_\infty}; \psi^* = \frac{\psi}{\psi_\infty}; \beta^* = \frac{\beta L_\infty}{\alpha_\infty}; \mathbf{u}^* = \frac{\mathbf{u}L}{\alpha_\infty};$$
$$t^* = \frac{t\alpha_\infty}{L_\infty^2}; P^* = \frac{PL^2}{\rho\alpha_\infty^2}; T^* = \frac{T - T_\infty}{T_\infty}; \quad (11)$$

where

$$\alpha_\infty = \frac{k_\infty}{(\rho c_p)_\infty} \quad (12)$$

and the subscript ∞ indicates a reference quantity. Assuming $\phi_\infty = k_b T_\infty / ze$ and substituting the above scales, we obtain the non-dimensional form of the equations as:

Laplace equation:

$$\nabla.(\lambda^* \nabla \phi^*) = 0 \quad (13)$$

where $\lambda^* = \lambda / \lambda_\infty$

Poisson-Boltzmann equation:

$$\nabla.(\varepsilon^* \nabla \psi^*) = ka^2 \sinh\left(\frac{\psi^*}{T^* + 1}\right) \quad (14)$$

where

$$\varepsilon^* = \frac{\varepsilon}{\varepsilon_\infty}; \kappa a = \left(\frac{2n_0 z^2 e^2 L_\infty^2}{\varepsilon_\infty \varepsilon_0 k_b T_\infty}\right)^{\frac{1}{2}} \quad (15)$$

The non-dimensional form of the momentum equation is

$$\left(\frac{\partial \mathbf{u}^*}{\partial t} + \mathbf{u}^*.\nabla \mathbf{u}^*\right) = -\nabla P^* + \mathrm{Pr}\nabla.\tau^* + J \sinh\frac{\psi^*}{T^* + 1}\nabla\phi^* \quad (16)$$

where

$$\upsilon^* = \frac{\upsilon}{\upsilon_\infty}; J = \frac{2n_0 k_b T_\infty L_\infty^2}{\alpha_\infty^2 \rho}; \mathrm{Pr} = \frac{c_p \mu_\infty}{k_\infty};$$
$$\tau^* = \upsilon^* \left(\nabla \mathbf{u}^* + \nabla \mathbf{u}^{*T}\right) \quad (17)$$

Finally, the non-dimensional form of the energy equation may be written as

$$\left(\frac{\partial T^*}{\partial t^*} + \mathbf{u}^*.\nabla T^*\right) = \nabla(\alpha^* \nabla T^*) + Ju\lambda^* \left|\nabla \phi^*\right|^2 \quad (18)$$

where

$$\alpha^* = \frac{\alpha}{\alpha_\infty}; Ju = \frac{\lambda_\infty k_b^2 T_\infty}{k_\infty z^2 e^2}; \lambda^* = \frac{\lambda}{\lambda_\infty} \quad (19)$$

In the present work, the electrical conductivity, viscosity and thermal conductivity are assumed to be temperature dependent. The temperature dependent relationships are given as

The electrical conductivity of the electrolyte:

$$\lambda^*(T) = \frac{\lambda}{\lambda_\infty} = \left[1 + \gamma^* T - T_\infty\right] = \left[1 + \gamma^* T^* T_\infty\right] \quad (20)$$

where γ^* is the slope ($\gamma^* \approx 0.025$(Tang et al., 2004*b*)).

The temperature dependent viscosity for the fluid is given as

$$\upsilon^*(T) = \frac{\upsilon}{\upsilon_\infty} = \frac{0.00276}{\upsilon_\infty} \exp(1713.0/T) 1.0 \times 10^{-6} \quad (21)$$

and the temperature dependent thermal conductivity ratio for the fluid is

$$\alpha^* = \frac{k_f}{k_\infty} = (0.61 + 0.0012 T_\infty T) / k_\infty \quad (22)$$

and for the solid,

$$\alpha^* = \frac{k_s}{k_\infty} = (1.38 + 0.0013 T_\infty T) / k_\infty \quad (23)$$

The reference thermal conductivity, k_∞, used in this study is assumed to be the thermal conductivity of the electrolyte at the reference temperature.

The important non-dimensional parameters identified above include the Prandtl number, *Pr*, and the parameters *J*, *Ka* and *Ju*. As seen, these parameters are defined using properties of the fluid and geometry that are known *a priori* for the electrolyte and the geometry used. Thus, determining these parameters independent of each other is straight forward,

unlike many other scales commonly employed in the literature. Table 1 lists various parameters, reference quantities and their values.

2.2 Numerical Algorithm

It is clear from the previous section that the independent variable, time, appears in some equations but the equations governing the electric fields are time independent. Thus, we solve the electric field equations using a GMRES solver (Singh et al., 2008). To overcome standard difficulties, a fractional step algorithm involving three steps and the energy equation may be written as (asterisks are dropped from the non-dimensional equations for simplicity)

Table 1: EOF and Joule heating parameters

Parameter	Value
α_∞	$0.146\times10^{-6} m^2/s$
ε_∞	78.5
J	$0.1-220$(micro-channel size between $1\mu m$ to $100\mu m$)
Ju	$0-10^{-2}$(depending on the reference electrical conductivity)
κa	$10-80$
k_∞	$0.6138 W/mK$
λ_∞	$0.2 S/m$
υ_∞	$0.8666\times10^{-6}\ m^2/s$
$\phi_{in};\phi_{out}$	134.4; 0.0 (equal to an electric field of $11.679 kV/m$)
Pr	5.877
ζ	-3.7(corresponding dimensional value is $95mV$)
T_∞	$298K$

Step1: Intermediate momentum

$$\left(\frac{\Delta\tilde{\mathbf{u}}}{\Delta t}+\mathbf{u}^n.\nabla\mathbf{u}^n\right)=\mathrm{Pr}\,\nabla.\tau^{n+\theta_1} +J\sinh\left(\frac{\psi}{T+1}\right)^{n+\theta}\nabla\phi^{n+\theta} \quad (24)$$

where $\Delta\tilde{u}=\tilde{u}-u^n$ and $\tilde{u}$ is an intermediate velocity field.

Step2: Pressure calculation

$$(1-\theta_2)\left(\frac{1}{\beta^2}\right)^n\frac{\Delta P}{\Delta t}-\Delta t\nabla^2P^{n+\theta_2}=-\nabla.\tilde{\mathbf{u}} \quad (25)$$

Step3: Momentum correction

$$\frac{\mathbf{u}^{n+1}+\tilde{\mathbf{u}}}{\Delta t}=-\Delta P^{n+\theta_2} \quad (26)$$

Energy equation:

$$\left(\frac{\Delta T}{\Delta t}+\mathbf{u}^n.\nabla T^n\right)=\nabla.(\alpha^*\nabla T^{n+\theta_1}) +Ju\left(\lambda|\nabla\phi|^2\right)^{n+\theta} \quad (27)$$

In the above equations θ_1 and θ_2 vary between 0 and 1 depending on whether equations are treated explicitly, implicitly or semi-implicitly. All the results given in the present work are generated by assuming $\theta=\theta_1=\theta_2=0$ (Arnold et al., 2008a; Arnold et al., 2008b; Nithiarasu, 2003; Nithiarasu et al., 2004; Nithiarasu, 2005; Zienkiewicz et al., 2005; Mynard and Nithiarasu, 2008; Nithiarasu et al., 2007). The finite element method is used for the spatial discretization of Equations (24) – (27).

3. Some Benchmark Solutions

The numerical model has been validated in many of our previous publications (Arnold et. al., 2008a; Arnold et al., 2008b; Singh et al., 2008). For the sake of completeness, a comparison between the numerical and analytical solutions for flow through a rectangular channel of non-dimensional width unity and length 10 is presented here. Figures 1(a) and 1(b) show the EOF potential and velocity distributions. As seen the agreement between the numerical and analytical solutions is excellent for all K(= κa) values.

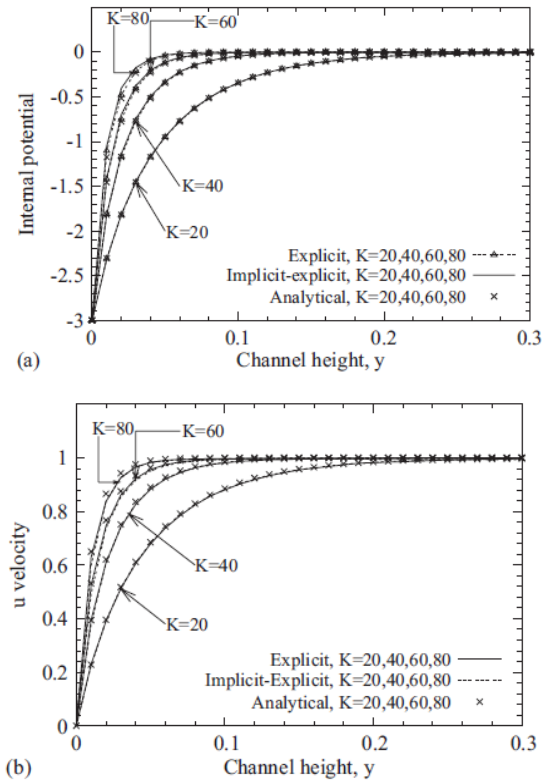

Figure 1 EOF through a rectangular channel (a) EOF potential (b) Velocity

4. A Conjugate Heat Transfer Problem

The problem considered here is shown in Figure 2. This is a conjugate heat transfer problem with convective heat transfer boundary condition at the top surface. The electrolyte is assumed to flow through the rectangular channel subjected to an external electric field along the channel. The temperature of the electrolyte entering the inlet is assumed to be at 298 K. Owing to the symmetry along the centre of the channel, only half of the geometry is used in the calculations as shown in Figure 2. The total length of the channel is ten times the channel width. The channel wall is assumed to be electrically insulated for the external potential and both the inlet and exit boundaries are assumed to have zero flux conditions for EOF potnetial. The non-dimensional velocity components on the solid walls are assumed to be zero and the horizontal velocity gradients at inlet and exit are also assumed to be zero. The cold fluid flowing into the channel is assumed to be at a non-dimensional temperature of zero (reference temperature). Apart from the top surface of the solid, the other two side surfaces of the solid part are assumed to be insulated (hatched sides in Figure 2). The fluid flow exit is also assumed to be insulated.

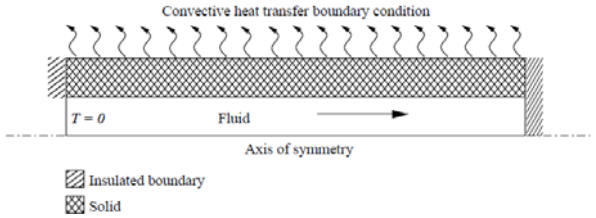

Figure 2 EOF and conjugate heat transfer in a channel. Domain and boundary conditions.

Figure 3 shows the distribution of electric potentials, velocity and temperature distribution. As seen the heat generated is convected along the top surface of the channel. The temperature is attempting to reach a developed value towards the exit of the channel.

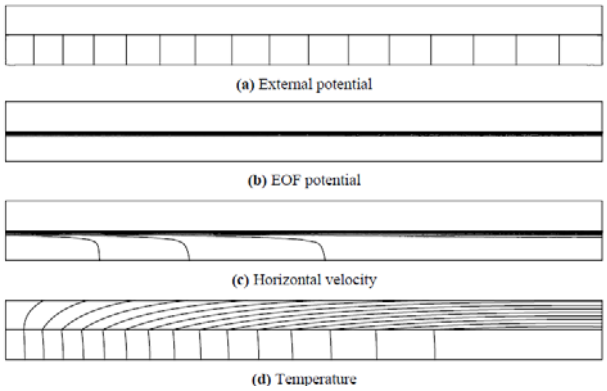

Figure 3 EOF and conjugate heat transfer in a channel. Contours of external potential, EOF potential, velocity and temperature Ju = 0.00001, Bi = 10.

Figure 4 shows the temperature profiles at different distances along the length of the channel. As seen the temperature is approaching a constant value towards the exit where the heat transferred and heat generated are approximately equal. It is also noticed the temperature variation near the inlet is rapid compared to the inner portion of the channel. This is due to the rapid heat transfer at the inlet and also relatively limited heat transfer area

available on the top surface near the inlet.

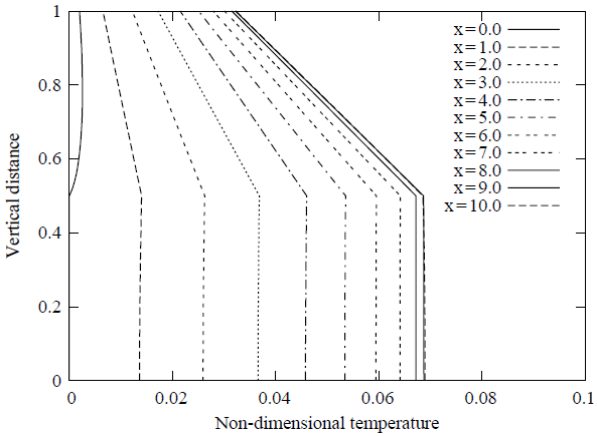

Figure 4 EOF and conjugate heat transfer in a channel. Temperature distribution at different sections of the channel, Ju = 0.00001, Bi = 10.

5. Heat Generation in a T-Mixer

EOF and heat generation in a two-dimensional T-mixer is studied here. The total length and width of the mixer are ten times the width of the inlet or exit sections. The mixer is symmetric with respect to the vertical central axis. The electrolytes used at the two horizontal inlets are assumed to be identical for demonstration purposes. All the other properties used are given in Table 1. Figure 5 shows the details of the mesh used in the vicinity of the T-junction.

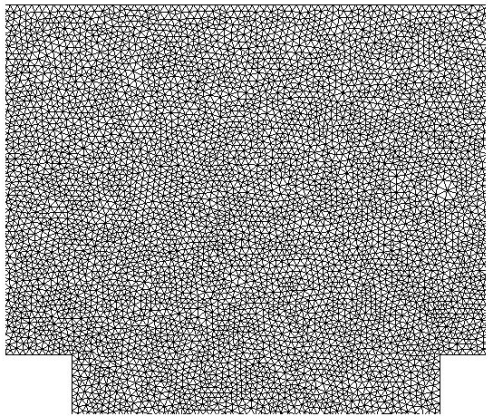

Figure 5 EOF and Joule heating in a T-mixer. Details of the unstructured mesh used near the T-junction.

A total of more than one hundred thousand finite elements are used to generate the mesh. The temperature boundary conditions used are zero non-dimensional temperature at the inlet and insulated boundary conditions on all the remaining surfaces including the exit. All the walls are prescribed with a constant zeta potential vale and an external electric field is introduced between the inlets and exit.

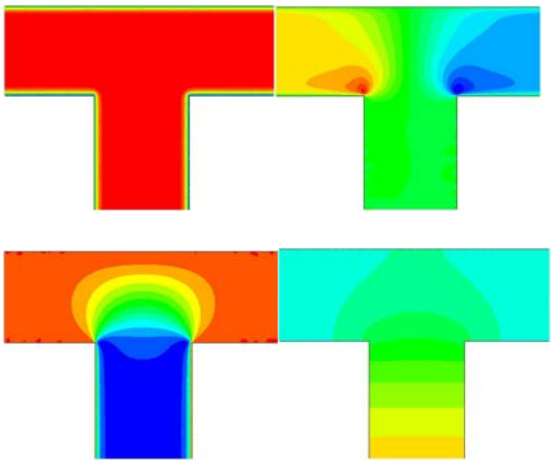

Figure 6 EOF and Joule heating in a T-mixer. Clockwise from the top left: EOF potential, horizontal velocity component, temperature and vertical velocity component.

Figure 6 shows the contours of EOF potential, velocity components and the temperature. As expected the distribution of variables is symmetric with respect to the vertical central axis due to the identical electrolytes assumed at both the horizontal exits. The arms of the T-mixer are dominated by the horizontal velocity component and the leg is dominated by the vertical component of the velocity field. The high EOF potential gradient clearly introduces a very high velocity gradient all along the walls of the T-mixer. The full details of the temperature distribution are shown in Figure 7. It is clear that the temperature gradient is large immediately after the junction towards the downstream of the mixer. In addition to the given parameter in Table 1, a Ju value of 0.00001 is used in the calculation. The increase in temperature for the above parameters is approximately 0.8^{o}C. Any further increase in Ju value will further increase the temperature and may results in damaging the electrolyte solution or the mixer.

A previous study (Nithiarasu and Lewis, 2009) clearly shows that for a simple and shorter channel flow, an order of magnitude increase in the *Ju* value increases the temperature to over 3^{o}C above the initial temperature.

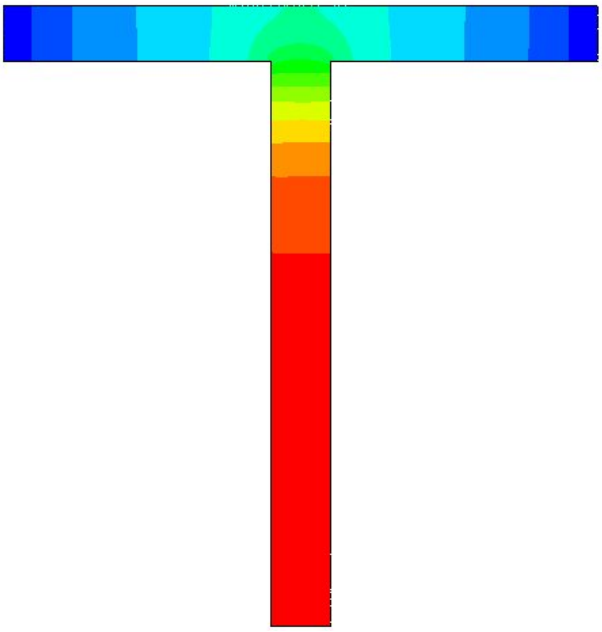

Figure 7 EOF and Joule heating in a T-mixer. Temperature distribution over the full domain.

6. Conclusions

A detailed modeling procedure for dealing with EOF based Joule heating was explained. The non-dimensional scales used are clearly an improvement over the existing scales. The formulation shows that the parameter *Ju* is the most important parameter in determining the heat generation.

References

Arnold, A.K. (2007), 'Numerical modelling of electroosmotic flows in micro-channels', *PhD Thesis*, Swansea Univeristy, UK.

Arnold, A.K., Nithiarasu, P. and Eng, P.F. (2008a), 'Electro-osmotic flow (eof) in microchannels', *Institution of Mechanical Engineers, Part C, Journal of Mechanical Engineering Science* 222, 753-759.

Arnold, A.K, Nithiarasu, P. and Tucker, P.G (2008b), 'Finite element modelling of electroosmotic flows using unstructured meshes', *International Journal of Numerical Methods for Heat and Fluid Flow* 18, 67-82.

Bianchi, F., Ferrigno, R. and Girault, H.H. (2000), 'Finite element simulation of an electroosmotic-driven flow division at a t-junction of microscale dimensions', *Analytical Chemistry* 72, 1987-1993.

Chein, R., Yang, Y.C. and Liu, Y. (2006), 'Estimation of joule heating effect on temperature and pressure distribution in electrokinetic-driven microchannel flows', *Electrophoresis* 27, 640-649.

Dutta, P. and Beskok, A. (2001), 'Analytical solution of mixed electroosmotic /pressure driven flows in two dimensional straight channels: Finite double layer effects', *Journal of Analytical Chemistry* 73, 1979-1986.

Erickson, D., Sinton, D. and Li, D. (2003), 'Joule heating an heat transfer in poly(dimethylsiloxane) microfluidic systems', *Lab on a Chip* 3, 141-149.

Huang, K.-D. and Yang, R.-J. (2006), 'Numerical modelling of the joule heating effect on electrokinetic flow focusing', *Electrophoresis* 27, 1957-1966.

Jiang, L., Mikkelsen, J., Koo, J.-M., Huber, D., Yao, S., Zhang, L., Zhou, P., Maveety, J.G., Prasher, R., Santiago, J.G., Kenny, T.W. and Goodson, K.E. (2002), 'Closed-loop electroosmotic microchannel cooling system for vlsi cirsuits', *IEEE Transactions on Components and Packaging Technologies* 25, 347-355.

Mynard, J.P. and Nithiarasu, P. (2008), 'A 1d arterial blood flow model incorporating ventricular pressure, aortic valve and regional coronary °ow using the locally conservative galerkin (lcg) method', *Communications in Numerical Methods in Engineering* 24, 367-417.

Nithiarasu, P. (2003), 'An effcient artificial compressibility (ac) scheme based on the characteristic based split (cbs) method for incompressible flows', *International Journal for Numerical Methods in Engineering* 56, 1815-1845.

Nithiarasu, P. (2005), 'An arbitrary Lagrangian Eulerian (ale) method for free surface flows using the characteristic based split (cbs) scheme', *International Journal for Numerical Methods in Fluids* 48, 1415-1428.

Nithiarasu, P. (2008), 'A unified fractional step method for compressible and incompressible flows, heat transfer and incompressible solid mechanics', *International Journal of Numerical Methods for Heat and Fluid Flow* 18, 111-130.

Nithiarasu, P. and Lewis, R.W., (2008), A short note on Joule heating in electroosmotic flows. A consistent non-dimensional scaling, *International Journal of Numerical Methods for Heat and Fluid Flow* 18, 919-931.

Nithiarasu, P., Liu, C.-B. and Massarotti, N. (2007), 'Laminar and turbulent flow calculations through a model human upper airway using unstructured meshes', *Communications in Numerical Methods in Engineering* 23, 1057-1069.

Nithiarasu, P., Mathur, J.S., Weatherill, N.P. and Morgan, K. (2004), 'Three-dimensional incompressible flow calculations using the characteristic based split (cbs) scheme', *International Journal for Numerical Methods in Fluids* 44, 1207-1229.

Nithiarasu, P., Seetharamu, K.N. and Sundararajan, T. (1998), 'Finite element analysis of transient natural convection in an odd-shapped enclosure', *International Journal of Numerical Methods for Heat and Fluid Flow* 8, 199-216.

Singh, S.P., Nithiarasu, P., Eng, P.F., Lewis, R.W. and Arnold, A.K. (2008), 'An implicit-explicit solution method for coupled electroosmotic flows in three dimensions using unstructured meshes', *International Journal for Numerical Methods in Engineering* 73, 1137-1152.

Tang, G., Yan, D., Yang, C., Gong, H., Chai, J. and Lam, Y. (2006), 'Assessment of joule heating and its effects on electroosmotic flow and electrophoretic transport of solutes in microfluidic channels', *Electrophoresis* 27, 628-639.

Tang, G.Y., Yan, D.G., Yang, C., Gong, H.Q., Chai, J.C. and Lam, Y.C. (2007), 'Joule heating and its effect on electrokinetic transport of solutes in rectangular microchannels', *Sensors and Actiators* 139, 221-232.

Tang, G.Y., Yang, C., Chai, C.J. and Gong, H.Q. (2003), 'Modeling of electroosmotic flow and capillary electrophoresis with the joule heating effect: The nernst-planck equation versus the boltzmann distribution', *Langmuir* 19, 10975-10984.

Tang, G.Y., Yang, C., Chai, C.K. and Gong, H.Q. (2004*a*), 'Joule heating effect on electroosmotic flow and mass species transport in a microcapillary.', *International Journal of Heat and Mass Transfer* 47, 215-227.

Tang, G.Y., Yang, C., Chai, C.K. and Gong, H.Q. (2004*b*), 'Numerical analysis of the thermal effect on electroosmotic flow and electrokinetic mass tranport in microchannels', *Analytica Chimica Acta* 507, 27-37.

Xuan, X., Sinton, D. and Li, D. (2004), 'Thermal end effects on electroosmotic flow in a capillary', *International Journal of Heat and Mass Transfer* 47, 3145-3157.

Zeng, S., Chen, C.-H., Mikkelsen Jr., J.C. and Santiago, J.G. (2001), 'Fabrication and characterization of electroosmotic micropumps', *Sensors and Actuators B* 79, 107-114.

Zhao, T.S. and Liao, Q. (2002), 'Thermal effects on electroosmotic pumping of liquids in Microchannels', *Journal of Micromechanics and Microengineering* 12(6), 962-970.

Zienkiewicz, O.C., Taylor, R.L. and Nithiarasu, P. (2005), *The finite element method for fluid dynamics*, Elsevier Butterworth-Heinemann, Elsevier Butterworth-Heinemann, Burlinton, MA.